Optimal Charging of Vehicle-to-Grid Fleets via PDE Aggregation Techniques

Caroline Le Floch, Florent di Meglio, and Scott Moura

***Abstract*— This paper examines modeling and control of a large population of grid-connected plug-in electric vehicles (PEVs). PEV populations can be leveraged to provide valuable grid services when managed via model-based control. However, such grid services cannot sacrifice a PEV's primary purpose – mobility. We consider a centrally located fleet of identical PEVs that are distributed to and collected from drivers. The fleet also provides regulation services to the grid, contracted a priori. We develop a partial differential equation (PDE)-based technique for aggregating large populations of PEVs. In particular, the model is a set of two first-order hyperbolic PDEs coupled with an ODE in time. PDE methods are of particular interest, since they provide an elegant modeling paradigm with a broad array of analysis and control design tools. The control design task is to minimize the cost of PEV charging, subject to supplying PEVs to drivers with sufficient charge and supplying the requested power to the grid. We examine this control design on a simulated case study, and analyze sensitivity to a variety of assumptions and parameter selections.**

I. Introduction

PEVs provide a compelling opportunity for supplying demand-side management services in the smart grid. Namely, a vehicle-to-grid (V2G) capable PEV communicates with the grid, stores energy, and can return energy to the electric grid. If properly managed, PEVs can enhance energy infrastructure resilience, enable renewable integration, and reduce economic costs for consumers and energy providers [1]. In addition to these societal-level infrastructure and environmental benefits, V2G may provide additional revenue streams to PEV owners [2]. Underscoring this opportunity, U.S. personal vehicles are parked and un-used 96% of time [3]. A single PEV can generally provide 5-20 kW, which is insufficient to participate in power grid markets. However, populations of PEVs can be aggregated to collectively provide grid services [4]. The main challenge, however, is monitoring and managing a large population of distributed PEV resources without sacrificing their primary function of personal mobility. As such, this paper examines modeling and control of grid integrated PEV populations.

The V2G concept was popularized by Kempton [5] and demonstration projects are underway [6]. Researchers are exploring many aspects of V2G, ranging from bi-directional power converters to public policy and energy market economics (see survey article [7]). A growing body of literature addresses design of smart charging algorithms for PEV control and examine various centralized or distributed protocols. Centralized algorithms [8], [9], require a central infrastructure to communicate with each agent, collect mobility information, and compute optimal load profiles for each PEV. When the number of agents grows, these methods require heavy communication, memory, and computational resources. In distributed optimization approaches each PEV solves a local problem and communicates independently to a central system. Recent studies have studied various distributed algorithms, including ADMM [10], non-cooperative games [11] and dual splitting [12]. However, for all these methods, the problem becomes harder to solve as the number of EVs grows: either the convergence time increases or the optimality of the computed solution decreases. In this paper we study a continuous modeling approach for PEV smart charging, as opposed to modeling each individual agent. Methods for modeling and controlling the population dynamics via PDEs have come into recent focus [13], [14]. The PDE system is subsequently discretized to formulate an aggregator control problem. Contrary to other methods, the our model complexity does not increase with the number of agents. In fact, model accuracy increases as the number of PEVs increases.

The remainder of this paper is organized as follows. Sections II and III develop and validate the PDE model of PEV aggregations. Section IV formulates the aggregator control problem, and Section V demonstrates the control results on an exemplary case study. Sensitivities to various modeling assumptions and parameters are provided in Section VI. Section VII summarizes the main results.

II. Modeling Aggregations of PEVs

We consider a fleet of identical PEVs managed by a central organization, where PEVs are checked-out to drivers. This context includes rental or car sharing fleets. We seek to model a large population of N individual PEVs as a continuous representation, mathematically represented by three coupled PDEs. PEVs in the population fall into three discrete states:

- *Charging*: a PEV receives energy from the grid (Grid-to-Vehicle or G2V)
- *Idle*: a PEV is plugged-in but does not charge, nor discharge.
- *Discharging*: a PEV supplies energy to the grid (Vehicle-to-Grid or V2G)

C. Le Floch and S. Moura are with the Energy, Controls, and Applications Laboratory (eCAL) in the Department of Civil and Environmental Engineering at the University of California, Berkeley, CA 94720, USA (e-mail: caroline.le_floch@berkeley.edu; smoura@berkeley.edu)

F. di Meglio is with the Centre Automatique et Systèmes, MINES ParisTech, 75272 Paris Cedex 06, France (e-mail: florent.di_meglio@mines-paristech.fr)

TABLE I

NOMENCLATURE

Symbol	Description
x	PEV battery SOE
t	Time
$u(x,t)$	Density of charging PEVs
$v(x,t)$	Density of idle PEVs
$w(x,t)$	Density of discharging PEVs
$\sigma_{i\to c}(x,t)$	Flow of PEVs from Idle to Charge
$\sigma_{i\to d}(x,t)$	Flow of PEVs from Idle to Discharge
$\sigma_{i\to Or}(x,t)$	Net Flow of PEVs from Idle to On Road
$Arr(x,t)$	Flow of PEVs from On Road to Idle
$Dep(x,t)$	Flow of PEVs from Idle to On Road
$q_c(x)$	Instantaneous charging power
$q_d(x)$	Instantaneous discharging power
X_{dep}	Min allowed SOE for departing PEVs
X_{max}	Min SOE for discharging and idle PEVs
X_{min}	Max SOE for charging cars
N_{min}	Min number of departure-ready PEVs at T_{max}

Each discrete state will be described by a transport PDE. The aggregator controls how PEVs switch from one discrete state to another. This ultimately renders coupling terms and forms a system of three coupled transport PDEs.

A. PDE Model

Consider a large population of plugged-in PEVs over the State of Energy (SOE) interval $[0,1]$ at some fixed time, as visualized by Fig. 1. PEVs exist in three states: charge $u(x,t)$, idle $v(x,t)$, and discharge $w(x,t)$. The σ terms model PEVs moving between individual states $\sigma_{i\to c}, \sigma_{i\to d}$, and between states and the environment, i.e. checked-in or out by drivers on the road $\sigma_{i\to Or}$. The cars, which are on road (uncontrollable) are not modeled in this framework; only the flow $\sigma_{i\to Or}$ is included.

To derive this aggregated PDE population model, we consider a simple PEV battery model. Denote the i'th PEV battery SOE and power by $x_i(t)$ and $P_i(t)$, respectively. Then a simple battery model is given by

$$\dot{x}_i(t) = \frac{\eta^m(x_i)}{E_{\max}} P_i(t), \qquad i = 1,\cdots,N, \tag{1}$$

$$m = \begin{cases} 1 & \text{if } P_i(t) \geq 0, \\ -1 & \text{if } P_i(t) < 0, \end{cases} \tag{2}$$

where $E_{\max}, \eta(\cdot), N$ are parameters that represent the battery energy capacity, power conversion efficiency, and PEV population size. Efficiency $\eta(\cdot) \in [0,1]$ is generally a function of SOE x_i. We assume $E_{\max}$ and $\eta(\cdot)$ are homogeneous across the entire population. Furthermore, the cumulative power consumption from charging and power generation from discharging is given, respectively, by

$$P_c(t) = \sum_{i=1}^{N} P_i \cdot \mathbb{1}(P_i > 0), \quad P_d(t) = \sum_{i=1}^{N} P_i \cdot \mathbb{1}(P_i < 0), \tag{3}$$

where $\mathbb{1}(\cdot)$ is the indicator function. More complex battery models could be considered in future work.

Let $u(x,t), v(x,t), w(x,t)$, all defined on the spaces $[0,1] \times \mathbb{R}^+ \to \mathbb{R}$, denote the PEV distribution at SOE x and time t, in the charging, idle, and discharging states, respectively. Consider an infinitesimal segment of $u(x,t)$ as shown in Fig.

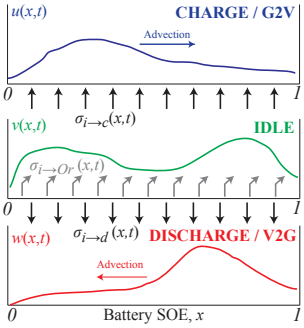

Fig. 1. PDE modeling concept for PEV populations.

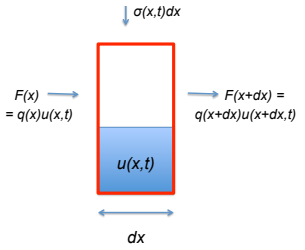

Fig. 2. Flows between x and $x+dx$

2. The number of charging PEVs at SOE level x at time t is denoted by $u(x,t)$. We seek to model the evolution of loads in the infinitesimal volume contained between x and $x+dx$. The PEVs with SOE x charge at rate $q_c(x,t) = \eta(x)/E_{\max} \cdot P(t)$. The entering flow and exiting flow are respectively:

$$F(x,t) = q_c(x,t)u(x,t), \tag{4}$$

$$F(x+dx,t) = q_c(x+dx,t)u(x+dx,t). \tag{5}$$

An additional flow of PEVs from the idle state to charging state are denoted $\sigma_{i\to c}(x,t)$ (see Fig. 1 and 2). During the infinitesimal time interval dt, the conservation law gives:

$$[u(x,t+dt) - u(x,t)]dx = \tag{6}$$
$$q_c(x,t)u(x,t)dt - q_c(x+dx,t)u(x+dx,t)dt + \sigma_{i\to c}(x,t)dt.$$

When $dt \to 0$ and $dx \to 0$, the relation becomes:

$$\frac{\partial u}{\partial t}(x,t) = -\frac{\partial}{\partial x}[q_c(x,t)u(x,t)] + \sigma_{i\to c}(x,t). \tag{7}$$

PDEs for the idle and discharging are similarly derived as

$$\frac{\partial v}{\partial t}(x,t) = -\sigma_{i\to or}(x,t) - \sigma_{i\to c}(x,t) - \sigma_{i\to d}(x,t), \tag{8}$$

$$\frac{\partial w}{\partial t}(x,t) = \frac{\partial}{\partial x}[q_d(x,t)w(x,t)] + \sigma_{i\to d}(x,t). \tag{9}$$

B. Boundary Conditions

For the system to be well posed, we need to define boundary conditions at $x=0$ for $u(x,t)$ and $x=1$ for $w(x,t)$. In addition, we must define boundary values for $q_c(x,t)$ and $q_d(x,t)$ to ensure physical meaning and conservation of loads in the system. Namely,

- The number of charging PEVs at SOE $x=0$ is zero, i.e. $u(0,t)=0$. No charging at $x=1$, i.e. $q_c(1,t)=0$.
- The number of discharging PEVs at SOE $x=1$ is zero, i.e. $w(1,t)=0$. No discharging at $x=0$, i.e. $q_d(0,t)=0$.

C. Discretization

The model is discretized using a high-resolution scheme with a Superbee flux limiter adapted to variable-coefficient linear transport equations from [15, Ch. 9, S. 4]. Practically, this is an upwind scheme with high-resolution corrections that provide second-order accuracy in space.

III. Model validation

A. V2G-Sim

We assess the aggregate PDE model's accuracy against the Vehicle-to-Grid Simulator (V2G-Sim) developed by the Grid Integration Group at Lawrence Berkeley National Laboratory [16]. V2G-Sim is an agent-based simulator that models the driving and charging behavior of individual PEVs and their grid impact. The necessary inputs for V2G-Sim are vehicle characteristics (e.g., battery capacity, battery charging model, powertrain parameters), driving schedules (e.g. duration of activities and drive cycles), and charging infrastructure (e.g. location of chargers, charging rate). The simulator is initialized with statistical data for trip length, departure times, and destination types derived from the 2009 National Household Travel Survey (NHTS) [17].

B. Validation method

The 2009 NHTS dataset includes trips from 17,805 vehicles in California during a weekday. We study four cases, which differ with respect to charging rates and control algorithms. PEV parameters are adopted from the Nissan Leaf with a battery energy capacity 26.8 kWh.

The first control algorithm is the standard open-loop strategy: vehicles begin to charge as soon as they plug in, and stop when they are fully charged. The second control algorithm includes V2G services. We apply a rudimentary V2G control algorithm to validate the PDE model: every PEV discharges during peak hours (6pm to 9pm) if it has sufficient charge ($SOE > 0.6$) and PEVs stop charging if $SOE > 0.55$. This algorithm is applied simply to evaluate the PDE model.

We assume the charging/discharging power is constant with respect to SOE, which is valid for the low battery C-rates (normalized charge rates) considered here. We study two charging rates: Level 1 (1.44 kW) and Level 2 (6.6 kW).

C. Validation results

We test our model for a 24 hour period in four different cases: $\{\text{L1 charger, L2 charger}\} \times \{\text{open loop, V2G control}\}$. In every case, we use a 0.01 SOE step. Since we need to satisfy the Courant Friedrichs Lewy (CFL) condition $\frac{qdt}{dx} \leq 1$ [15], time step sizes differ for L1 and L2 chargers: 11.4 minute interval for L1 chargers (120 time steps) and a 2.4 minute interval for L2 chargers (601 time steps).

We compute the $\mathscr{L}_2$ norm of the difference between the PDE model and the V2G-Sim distribution as

$$e(t) = \frac{||(u+v+w)_{PDE}(\cdot,t) - (u+v+w)_{V2Gsim}(\cdot,t)||_2}{||(u+v+w)_{V2Gsim}(\cdot,t)||_2}, \tag{10}$$

where f_{PDE} refers to the values from the aggregated PDE model and f_{V2Gsim} refers to V2G-Sim.

Table II provides the average normalized error over the 24 hour period. The PDE model approximates the SOE distributions with an average normalized error of less than 3% and is more accurate for the open loop cases. Figure 3 shows $e(t)$ for each time step. For both L1 cases and the open-loop L2 case, $e(t)$ is always less than 10%. For L2 chargers with V2G, Fig.3 shows that $e(t)$ has large values for some isolated time steps. These "spikes" only occur during the discharging period (from 6pm to 9pm) and have similar magnitudes. These errors are in fact a numerical artifact of the PDE discretization technique. Namely, at the end of the charging period (6pm), PEVs tend to be aggregated at the maximum allowable SOE. When PEVs discharge, then this peak transports toward 0% SOE. This is highlighted in Fig. 5, which show snapshots of the distributions immediately before, during, and immediately after the V2G period, for the PDE model and V2G-Sim. The numerical phenomenon occurs when there is a one SOE-step difference between the load peaks in V2G-Sim and the PDE model. This can be resolved via SOE smoothing. Figure 3 shows the smoothed error $e_{smooth}(t)$ (in green) after averaging the load distribution with the two closest SOE steps. The smoothed error $e_{smooth}(t)$ is smaller than 4% for every time step.

TABLE II
Mean Normalized Error over Time

Case	$1/T \cdot \int_0^T e(t)dt$
L1 Open Loop	0.011
L1 V2G	0.023
L2 Open Loop	0.002
L2 V2G	0.028

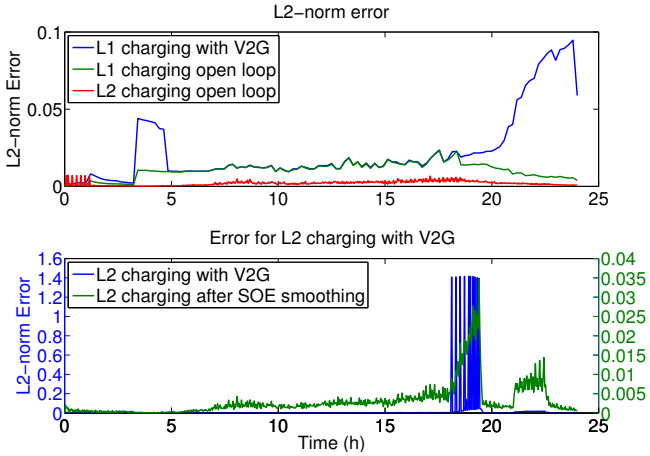

Fig. 3. Error in the 4 different scenarios

$$e_{smooth}(t) = \frac{||(u_a+v_a+w_a)_{PDE}(\cdot,t) - (u_a+v_a+w_a)_{V2Gsim}(\cdot,t)||_2}{||(u_a+v_a+w_a)_{V2Gsim}(\cdot,t)||_2}, \tag{11}$$

where $g_a(x,t) = \frac{g(x-dx,t)+g(x,t)+g(x+dx,t)}{3}$.

The aggregated charging and discharging power is provided in Fig. 4. The aggregated PDE provides excellent accuracy, even in the case of L2 charging with V2G control. Thus, the PDE model predicts aggregated fleet charge and discharge sufficiently well, despite small offsets in time or SOE due to numerical implementation. In the next section, we use this PDE formulation to design a control algorithm to optimally schedule EV charging and discharging.

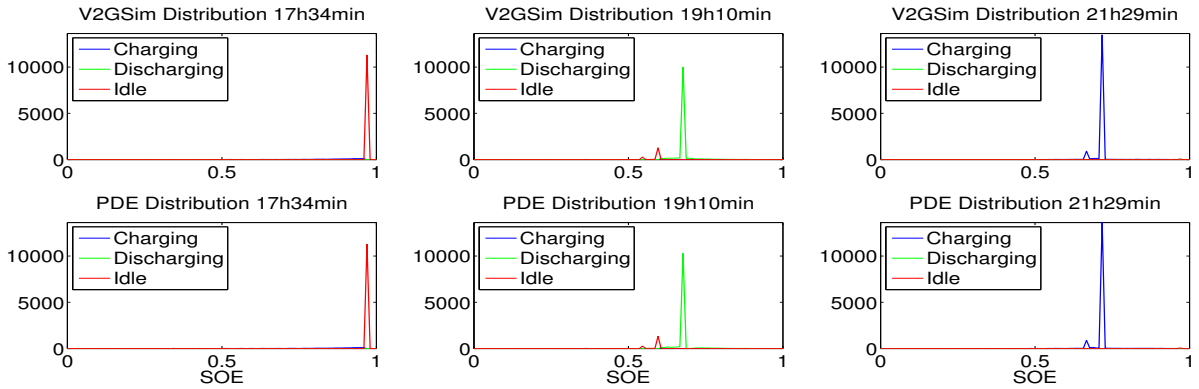

Fig. 5. PEV distributions immediately before, during, and after V2G event for the PDE model and V2G-Sim. Large errors occur due to distribution peaks that are slightly offset in SOE (or time) between two models. This numerical error has relatively no impact for our control purposes.

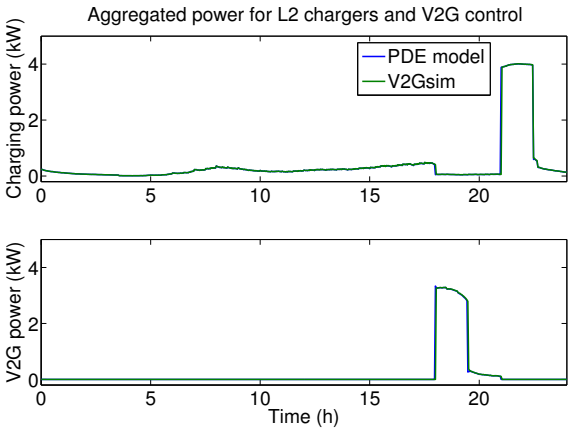

Fig. 4. Aggregated Power for L2 charger and V2G control

IV. Optimal control formulation

The control objective is to minimize the cost of charging PEVs, subject to supplying sufficient energy to the grid (for services contracted *a priori*) and providing sufficiently charged EVs to drivers. We make the following assumptions:

(A1) The cost of electricity $C_{elec}(t)$ is known in advance.
(A2) EVs must be provided to drivers with a minimum required State of Energy (SOE), X_{dep}.
(A3) The driver demand for vehicles is known in advance.
(A4) The aggregator sells energy to the regulation market. It bids $P^{des}(t)$ one day in advance.

The real time regulation signal might be lower than $P^{des}(t)$. However, the optimization program seeks a robust control, which ensures that the aggregator has the available power capacity during the entire day.

A. Optimal problem

The aggregator minimizes the cost of charging vehicles over finite time period $t \in [0, T_{max}]$.

$$C = \int_0^{T_{max}} C_{elec}(t) \int_0^1 q_c(x,t)u(x,t)\ dx\ dt, \qquad (12)$$

where only the charging state $u(x,t)$ appears explicitly. To ensure physical meaning of the system, we also impose boundaries on SOE values for each category. For $x > X_{max}$, cars are restricted from charging further and for $x < X_{min}$, cars are forced to charge:

$$u(x,t) = 0, \qquad \forall\ x \geq X_{max}, \qquad (13)$$
$$v(x,t) = 0 = w(x,t), \qquad \forall\ x \leq X_{min}, \qquad (14)$$

The system must also satisfy three additional constraints.

1) Power supply constraint: We consider a scenario where the EV aggregator participates in a regulation market. We assume the bidding process has been completed and the system operator has assigned an available frequency up regulation capacity. Hence, the V2G aggregator commits to supply at least $P^{des}(t)$:

$$\int_0^1 q_d(x)w(x,t)dx \geq P^{des}(t), \quad \forall\ t. \qquad (15)$$

2) Drivers' demand constraint: We assume the demand and arrival of cars are known in advance. This could be true in a reservation-based system. This assumption is admittedly restrictive, and will be examined via a sensitivity analysis in Section VI. The arrival of cars $Arr(x,t)$ is known for all time and all SOE values. Similarly the total demand of vehicles over time $Dem(t)$ is known one day in advance. The aggregator decides which PEVs are vended to the drivers, i.e. at what SOE. In addition, we require vended PEVs to have a minimum SOE level X_{dep} upon departure. Then, $Dep(x,t)$ becomes a controllable input, which satisfies the following constraint:

$$\int_{X_{dep}}^1 Dep(x,t)\ dx = Dem(t), \quad \forall\ t. \qquad (16)$$

3) Time horizon and final condition: Note that we consider a finite-time horizon optimization problem. To ensure continuity of the system after time period T_{max}, we require that the system contains a minimum number of PEVs N_{min} that are able to depart after T_{max}.

$$\int_{X_{dep}}^1 (u+v+w)(x,T_{max})\ dx \geq N_{min}. \qquad (17)$$

B. Formulation of the optimization problem

The optimization problem is summarized as

$$\min_{\sigma_{i\to d},\sigma_{i\to c},Dep} C = \int_0^{T_{max}} C_{elec}(t) \int_0^1 q_c(x,t)u(x,t)\ dx\ dt, \quad (18)$$

subject to: (7), (8), (9),

$$u(0,t) = 0,\ w(1,t) = 0, \quad (19)$$

$$u(x,0) = u_0(x),\ v(x,0) = v_0(x),\ w(x,0) = w_0(x), \quad (20)$$

$$-w(x,t) \le \sigma_{i\to d}(x,t) \le v(x,t), \quad (21)$$

$$-u(x,t) \le \sigma_{i\to c}(x,t) \le v(x,t), \quad (22)$$

(13) − (17).

Note all the functions and constraints are linear with respect to states u, v, w, rendering a linear program.

To generate a finite dimensional linear program, we discretize the PDEs. Denote $n \in [0,N]$ as the index for time with time step Δt, $T_{max} = N\Delta t$. Denote $j \in [0,J]$ as the index for SOE with step Δx. Spatio-temporally dependent variables are discretized into the form $f_j^n = f(j\Delta x, n\Delta t)$. We denote M_c and M_d as the transition matrices derived from discretization of PDEs (see Section II-C). The PDE dynamics are then approximated by:

$$u^{n+1} = M_c u^n + \sigma_{i\to c}^{n+1}, \quad (23)$$

$$v^{n+1} = v^n - [\sigma_{i\to c}^{n+1} + \sigma_{i\to d}^{n+1} + \sigma_{i\to Or}^{n+1}], \quad (24)$$

$$w^{n+1} = M_d w^n + \sigma_{i\to d}^{n+1}. \quad (25)$$

We arrive at an explicit linear formulation after eliminating the control variables $\sigma_{i\to d}$ and $\sigma_{i\to c}$ and expressing everything in terms of u, v, w. The optimization problem becomes

$$\min_{u,v,w,Dep} \Delta t\ \Delta x \sum_{n=0}^{N}\sum_{j=0}^{J} C_{elec}^n q_j^n w_j^n \quad (26)$$

subject to

$$[u+v+w]^{n+1} + \frac{Dep^{n+1}}{\Delta x} = M_c u^n + M_d w^n + \frac{Arr^{n+1}}{\Delta x} \quad (27)$$

$$u_0^n = 0, \quad v_J^n = 0, \quad (28)$$

$$u_j^0 = u_0(j\Delta x),\ v_j^0 = v_0(j\Delta x),\ w_j^0 = w_0(j\Delta x),\ \forall j, \quad (29)$$

$$u^n, v^n, w^n, Dep^n \ge 0, \quad (30)$$

$$u_j^n = 0\ \forall\ j \ge X_{max}\cdot J \quad (31)$$

$$v_j^n = 0 = w_j^n\ \forall\ j \le X_{min}\cdot J \quad (32)$$

$$\Delta x \sum_{j=0}^{J} q_{d,j}^n w_j^n \ge P^{des,n} \quad (33)$$

$$\sum_{j=X_{dep}\cdot J}^{J} Dep_j^n = Dem^n \quad (34)$$

$$\Delta x \sum_{j=X_{dep}\cdot J}^{J} u_j^N + v_j^N + w_j^N \ge N_{min} \quad (35)$$

The program is linear with respect to u, v, w, Dep and we use an off-the-shelf linear programming solver.

V. Results

A. Data

We extract daily trip data (departure and arrival time of vehicles) from the 2009 NHTS for 2,300 California vehicles

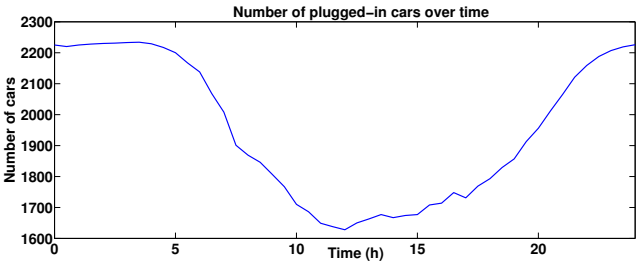

Fig. 6. Number of Plugged-in cars

[17]. Figure 6 shows the total number of plugged-in cars over one day. Vehicles have a 28.6 kWh capacity and are charged with L1 chargers (1.9kW). A 30 minute time step is used. Electricity price is taken from the California Independent System Operator (CAISO [18]) We use the electricity price on the Day-Ahead market for an arbitrarily selected weekday (August 22, 2014), from the local utility, PG&E (Fig. 7).

The regulation power $P^{des}(t)$ is generally defined on a hourly basis. That is, the aggregator bids a Contracted Power Capacity (*CPC*) and the System Operator provides orders for regulation up and down one day in advance. Due to uncertainties in the number of plugged-in cars and the required energy to satisfy drivers, determining a V2G *CPC* is an open question [6], [19]. One idea is to determine the Achievable Power Capacity (APC) from the number of plugged-in vehicles [19]. That is, $APC(t)$ is defined by the number of plugged-in PEVs (Fig. 6) and their discharging rate $q_d = 1.9kW$. $APC(t)$ provides the instantaneously available capacity and gives an upper bound for the fleet discharge power. Then a simple energy management method is to bid for a percentage $\alpha \in [0,1]$ of the *APC*,

$$CPC(t) = \alpha \cdot APC(t). \quad (36)$$

In the remainder of the paper we define $P^{des}(t) = \alpha \cdot APC(t)$ for different values of α. Remaining simulation parameters include: $X_{dep} = 0.75$, $X_{max} = 0.95$, $X_{min} = 0.2$, $N_{min} = 800$, $u(x,0) = 2225$, $v(x,0) = w(x,0) = 0$.

B. Optimal Charging

The control algorithm ultimately provides the distributions of PEVs between the three categories: Charging, Idle, and Discharging. Figure 7(a) presents the resulting distribution for $\alpha = 0.25$ and Fig. 7(b) shows V2G power and requested power during the day.

The controller ensures enough PEVs exist in discharging mode to meet the power supply demand (Fig. 7(b)). The remaining PEVs are managed between Charge and Idle to meet demand from drivers and to minimize overall cost (Fig. 7(a)). In this case study, PEVs mainly charge from 1 am to 3 pm, when the price of electricity is low. After 4pm large flows occur from Charge to Idle to avoid peak hour charging.

A second aspect of the controller is to optimize the distribution of cars along SOE values. Figure 8(a) shows how the controller tends to aggregate cars around particular SOE values. At the end of the optimization period, PEVs are mostly in the idle category and are charged at the

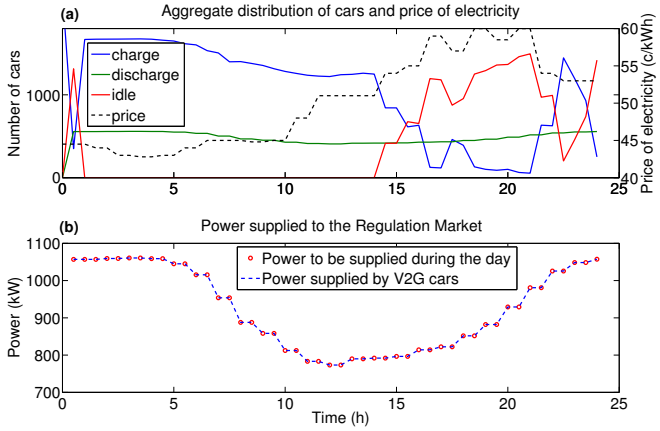

Fig. 7. Resulting distribution of vehicles and V2G power for $\alpha = 0.25$

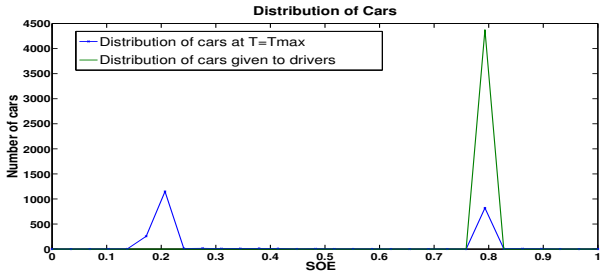

Fig. 8. Distribution of cars along SOE values

minimum required value $X_{min} = 0.2$. A second peak occurs at $X_{dep} = 0.75$, which corresponds to the final constraint of having a minimum number of cars $N_{min} = 800$ at T_{max}. The controller also optimizes the SOE level for departing cars, with respect to condition $x \geq X_{dep}$. Figure 8(b) shows that almost all cars depart with the minimum required SOE, X_{dep}.

VI. Sensitivity Analysis and Feasibility

A major assumption is that PEV arrivals and departures are known in advance. Even if statistical studies or reservation-based systems provide very good forecasts of driver behavior, it is impossible to have an exact prediction. Therefore, we investigate how the program reacts to uncertainties in driving schedules. In the optimization program detailed above, the demand for cars (*Dem* and *Arr*) impacts the constraints and does not impact the cost function. Therefore, if the actual demand is different from the expected one, then the cost will remain the same but constraints may be violated.

1) Higher demand than expected: We run the optimization with several parameters and various values for the expected demand. Then, we apply the resulting control signal with a higher demand than the expected one and examine the impact on the constraints. Simulations demonstrate that:

- The final constraint (17) is almost always violated. If the overall demand for cars is $D + \Delta D$ instead of D, then the available number of cars at T_{max} will be $N_{min} - \Delta D$ instead of N_{min}.
- The demand departure constraint $x \geq X_{dep}$ is never active in our simulations. Figure 9 shows how much the demand can increase before the departure constraint becomes active, for different values of α. Except for small values of α, the demand can double (more than 100% margin) without violating $x \geq X_{dep}$, thus demonstrating robustness to this particular constraint.

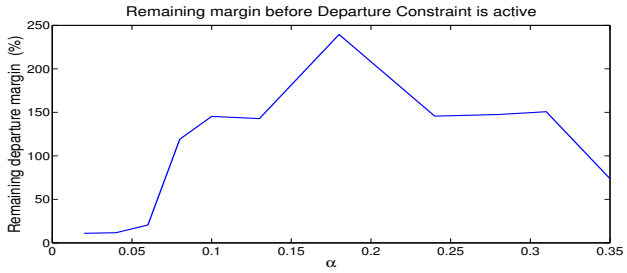

Fig. 9. Sensitivity analysis to higher demands

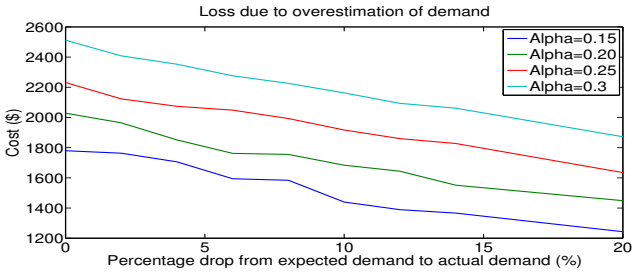

Fig. 10. Impact of lower than expected demand on cost.

2) Lower demand than expected: In this case, every constraint is satisfied but the solution is suboptimal. Since the aggregator overestimates the demand the resulting cost is higher. Figure 10 shows how the realized cost relates to the optimal cost for lower demands than expected.

3) Impact of control parameters on cost and feasibility: We examine two sets of parameters for the aggregator:

- α is a grid-related parameter. If α increases, the aggregator bids more power and V2G power increases.
- N_{min}, X_{dep} are driver-related parameters. If their values increase, SOE capacity offered to drivers increases.

Figure 11 shows the variability of cost with respect to variations in these three parameters and Fig. 12 shows the variability of cost per unit of V2G power ($/kWh). The graphs show how the parameters impact cost and feasibility of the system, and the tradeoffs in selecting these values.

- If α increases, then more power is necessary for the regulation up and the cost of PEV charging increases.
- If α, X_{dep} and N_{min} simultaneously take sufficiently high values, then the constraints are too restrictive and the problem becomes infeasible. High values of α imply less flexibility to keep energy for drivers.
- Figure 12 shows that the optimization program leads to economies of scale. Cost per kW decreases with increasing α. That is, the aggregator is more aggressive in utilizing excess PEV SOE for V2G services.

4) Impact of charging rate on cost and feasibility: The optimization program depends on the available charging infrastructure and especially charge/discharge rates $q_c(x,t), q_d(x,t)$. Figure 13 presents the results for different

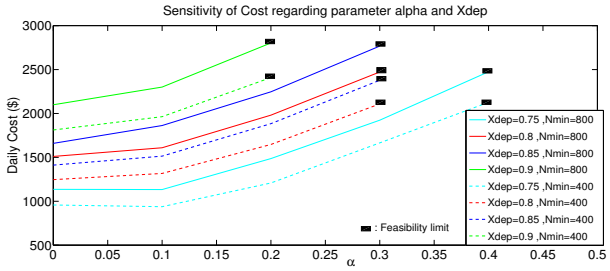

Fig. 11. Sensitivity analysis regarding α , X_{dep} and N_{min}

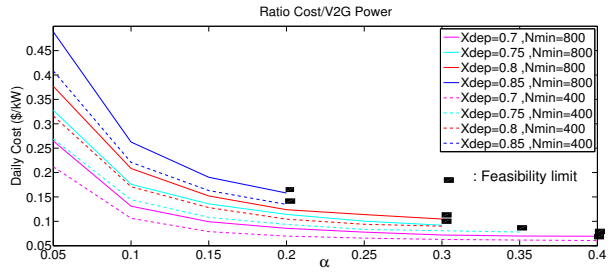

Fig. 12. Sensitivity analysis regarding α and X_{dep} and N_{min}

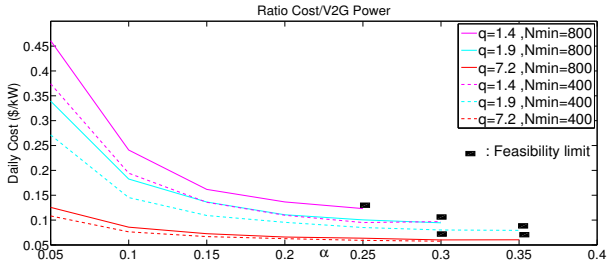

Fig. 13. Sensitivity analysis regarding α, q and N_{min}

rate values); fast charging allows more flexibility and higher instantaneous power. Cost per generated power is therefore lower with fast chargers and more stringent constraints can be satisfied.

VII. Conclusions

This paper develops a partial differential equation (PDE)-based model for grid-integrated plug-in electric vehicle (PEV) populations. The model consists of three coupled transport PDEs. We utilize this model to optimally manage the PEV fleet to: (i) deliver contracted grid services, (ii) supply drivers with sufficiently charged PEVs, and (iii) minimize charging costs. We examine a case study and assess sensitivity to uncertainties in PEV arrivals/departures, V2G service level, and mobility-related parameters. Future work will consider stochastic information for PEV arrivals, departures, electricity prices, and regulation signals in a real-time optimal control setting, such as stochastic model predictive control.

References

[1] D. B. Richardson, "Electric vehicles and the electric grid:a review of modeling approaches, impacts, and renewable energy integration," *Renewable Sustainable Energy Reviews*, vol. 19, pp. 247–254, 2013.

[2] W. Kempton and J. Tomić, "Vehicle-to-grid power fundamentals: Calculating capacity and net revenue," *Journal of power sources*, vol. 144, no. 1, pp. 268–279, 2005.

[3] A. Langton and N. Crisostomo, "Vehicle-grid integration: A vision for zero-emission transportation interconnected throughout california's electricity system," California Public Utilities Commission, Tech. Rep. R. 13-11-XXX, 2013.

[4] D. Callaway and I. Hiskens, "Achieving controllability of electric loads," *Proceedings of the IEEE*, vol. 99, no. 1, pp. 184–199, Jan. 2011.

[5] W. Kempton and S. E. Letendre, "Electric vehicles as a new power source for electric utilities," *Transportation Research Part D: Transport and Environment*, vol. 2, no. 3, pp. 157–175, 1997.

[6] W. Kempton, V. Udo, K. Huber, K. Komara, S. Letendre, S. Baker, D. Brunner, and N. Pearre, "A test of vehicle-to-grid (v2g) for energy storage and frequency regulation in the pjm system," *Results from an Industry-University Research Partnership*, p. 32, 2008.

[7] R. J. Bessa and M. A. Matos, "Economic and technical management of an aggregation agent for electric vehicles: a literature survey," *European Transactions on Electrical Power*, vol. 22, no. 3, pp. 334–350, 2012.

[8] K. Clement, E. Haesen, and J. Driesen, "Coordinated charging of multiple plug-in hybrid electric vehicles in residential distribution grids," in *Power Systems Conference and Exposition, 2009. PSCE '09. IEEE/PES*, March 2009, pp. 1–7.

[9] E. Sortomme, M. Hindi, S. MacPherson, and S. Venkata, "Coordinated charging of plug-in hybrid electric vehicles to minimize distribution system losses," *IEEE Transactions on Smart Grid*, vol. 2, no. 1, pp. 198–205, March 2011.

[10] J. Rivera, P. Wolfrum, S. Hirche, C. Goebel, and H.-A. Jacobsen, "Alternating direction method of multipliers for decentralized electric vehicle charging control," in *Decision and Control (CDC), 2013 IEEE 52nd Annual Conference on*, Dec 2013, pp. 6960–6965.

[11] Z. Ma, D. S. Callaway, and I. A. Hiskens, "Decentralized charging control of large populations of plug-in electric vehicles," *Control Systems Technology, IEEE Transactions on*, vol. 21, no. 1, pp. 67–78, 2013.

[12] L. Gan, U. Topcu, and S. H. Low, "Optimal decentralized protocol for electric vehicle charging," *Power Systems, IEEE Transactions on*, vol. 28, no. 2, pp. 940–951, 2013.

[13] S. Bashash and H. Fathy, "Transport-based load modeling and sliding mode control of plug-in electric vehicles for robust renewable power tracking," *Smart Grid, IEEE Transactions on*, vol. 3, no. 1, pp. 526–534, March 2012.

[14] S. Moura, J. Bendtsen, and V. Ruiz, "Parameter identification of aggregated thermostatically controlled loads for smart grids using pde techniques," *International Journal of Control*, vol. 87, no. 7, pp. 1373–1386, 2014.

[15] R. J. LeVeque, *Finite volume methods for hyperbolic problems*. Cambridge university press, 2002, vol. 31.

[16] V2g-sim. [Online]. Available: http://v2gsim.lbl.gov

[17] USDOT-FHWA, "National Household Travel Survey," U.S. Department of Transportation, Federal Highway Administration, Tech. Rep., 2009, http://nhts.ornl.gov/index.shtml.

[18] CAISO. Day-ahead daily market watch aug 22 2014. [Online]. Available: http://www.caiso.com/Documents/Day-AheadDailyMarketWatchAug222014.pdf

[19] S. Han, S. Han, and K. Sezaki, "Estimation of achievable power capacity from plug-in electric vehicles for v2g frequency regulation: Case studies for market participation," *Smart Grid, IEEE Transactions on*, vol. 2, no. 4, pp. 632–641, 2011.